

Mcl-1-dependent activation of Beclin 1 mediates autophagic cell death induced by sorafenib and SC-59 in hepatocellular carcinoma cells

W-T Tai^{1,2,8}, C-W Shiau^{3,8}, H-L Chen^{1,2}, C-Y Liu^{3,4,5}, C-S Lin⁶, A-L Cheng^{2,7}, P-J Chen^{1,2} and K-F Chen^{*,1,2}

We investigated the molecular mechanisms underlying the effect of sorafenib and SC-59, a novel sorafenib derivative, on hepatocellular carcinoma (HCC). Sorafenib activated autophagy in a dose- and time-dependent manner in the HCC cell lines PLC5, Sk-Hep1, HepG2 and Hep3B. Sorafenib downregulated phospho-STAT3 (P-STAT3) and subsequently reduced the expression of myeloid cell leukemia-1 (Mcl-1). Inhibition of Mcl-1 by sorafenib resulted in disruption of the Beclin 1-Mcl-1 complex; however, sorafenib did not affect the amount of Beclin 1, suggesting that sorafenib treatment released Beclin 1 from binding with Mcl-1. Silencing of SHP-1 by small interference RNA (siRNA) reduced the effect of sorafenib on P-STAT3 and autophagy. Ectopic expression of Mcl-1 abolished the effect of sorafenib on autophagy. Knockdown of Beclin 1 by siRNA protected the cells from sorafenib-induced autophagy. Moreover, SC-59, a sorafenib derivative, had a more potent effect on cancer cell viability than sorafenib. SC-59 downregulated P-STAT3 and induced autophagy in all tested HCC cell lines. Furthermore, our *in vivo* data showed that both sorafenib and SC-59 inhibited tumor growth, downregulated P-STAT3, enhanced the activity of SHP-1 and induced autophagy in PLC5 tumors, suggesting that sorafenib and SC-59 activate autophagy in HCC. In conclusion, sorafenib and SC-59 induce autophagy in HCC through a SHP-1-STAT3-Mcl-1-Beclin 1 pathway.

Cell Death and Disease (2013) 4, e485; doi:10.1038/cddis.2013.18; published online 7 February 2013

Subject Category: Cancer

Hepatocellular carcinoma (HCC) is the fifth most common cancer worldwide and the third leading cause of cancer death.¹ Incidence of HCC is strongly correlated with cirrhosis that results from causes such as chronic hepatitis B virus (HBV)^{2,3} and/or chronic hepatitis C virus (HCV) infection, aflatoxin exposure, alcoholic cirrhosis and cigarette smoking.^{1,4,5} As HCC is highly resistant to chemotherapy, targeted therapies have been evaluated as first-line treatments or combinational therapies.^{6–8} Sorafenib (Nexavar), a multiple kinase inhibitor, was approved by the US Food and Drug Administration for the treatment of advanced HCC in 2007, and is the first clinically approved targeted drug therapy for HCC.^{9,10} However, the precise mechanism by which sorafenib induces tumor cell death is still under investigation. We identified STAT3 as a major kinase-independent target of sorafenib through increasing SH2-containing protein tyrosine phosphatase (SHP-1) activity.^{11,12} SHP-1 is a key negative regulator of STAT3 that can dephosphorylate p-STAT3 and further inhibit its downstream gene expression.¹³ We validated the role of the SHP-1/STAT3-related signaling pathway in the sorafenib-induced anti-HCC effect by several novel kinase-independent derivatives of sorafenib.^{14,15} These

derivatives, which had no inhibitory effect on kinases such as the Raf and VEGFR families showed a similar or more potent antitumor effect than sorafenib through the activation of SHP-1 phosphatase activity.

Autophagy is an important catabolic process for the degradation of cytoplasmic proteins via autolysosomal digestion.^{16,17} Autophagy is initiated by the formation of a membranous cistern called the isolation membrane (or phagophore) that contains damaged cell components. Next, a nascent membrane is further fused to form a double-membrane vesicle (called an autophagosome). The process of mammalian autophagy is divided into six principal steps: initiation, nucleation, elongation, closure, maturation and degradation.^{16,18} In addition to degradation thorough lysosomal machinery, autophagy has been reported to induce programmed cell death called autophagic cell death (ACD, programmed cell death type II).^{19–21} Beclin 1 (Atg6), a Bcl-2-homology domain 3 (BH3) protein, interacts with Vps34 (a class III PI3K), Vps15 (a myristoylated kinase) and UV irradiation resistance-associated tumor suppressor gene (UVRAG) to form a core complex to allow autophagosome nucleation, a vital step of autophagy.²² However, Bcl-2 and

¹Department of Medical Research, National Taiwan University Hospital, Taipei, Taiwan; ²National Center of Excellence for Clinical Trial and Research, National Taiwan University Hospital, Taipei, Taiwan; ³Institute of Biopharmaceutical Sciences, National Yang-Ming University, Taipei, Taiwan; ⁴Division of Hematology and Oncology, Department of Medicine, Taipei Veterans General Hospital, Taipei, Taiwan; ⁵School of Medicine, National Yang-Ming University, Taipei, Taiwan; ⁶School of Veterinary Medicine, National Taiwan University, Taipei, Taiwan and ⁷Department of Oncology, National Taiwan University Hospital, Taipei, Taiwan

*Corresponding author: K-F Chen, Department of Medical Research, National Taiwan University Hospital, No 7, Chung-Shan South Road, Taipei 100, Taiwan.

Tel: +886 2 23123456, ext: 63548; Fax: +886 2 23225329; E-mail: kfchen1970@ntu.edu.tw

⁸These authors contributed equally to this work.

Keywords: SC-59; sorafenib; STAT3; HCC

Abbreviations: HCC, hepatocellular carcinoma; TRAIL, tumor necrosis factor-related apoptosis-inducing ligand; STAT3, signal transducers and activators of transcription 3; DMEM, Dulbecco's modified Eagle's medium; FBS, fetal bovine serum

Received 03.9.12; revised 05.1.13; accepted 09.1.13; Edited by A Rufini

Bcl-xL can interact with Beclin 1 via the BH3 domain and inhibit the Beclin 1-containing core complex. In addition, the expression level of myeloid cell leukemia-1 (Mcl-1) has been suggested to regulate autophagic flux. Specifically, deletion of Mcl-1 in cortical neurons of transgenic mice has been found to activate a robust autophagic response.²³ The inhibition of Mcl-1 is hypothesized to induce autophagic cell death.

In this study, we unraveled the molecular mechanism by which sorafenib induces autophagy in HCC cells. We found that sorafenib-induced degradation of Mcl-1 disrupts its association with Beclin 1 and promotes significant autophagic cell death. Using a kinase-independent derivative of sorafenib, SC-59, we confirmed that this autophagic effect is related to the SHP-1/STAT3 signaling pathway. Both SC-59 and sorafenib resulted in disassociation of the Mcl-1–Beclin 1 complex and induced autophagic cell death *in vitro* and *in vivo* via a SHP-1/STAT3-dependent mechanism.

Results

Sorafenib induces autophagy in HCC cell lines. Autophagy is known to be able to either suppress or promote cancer cell growth depending upon cell status. First, to evaluate the potential autophagic effect of sorafenib in HCC cells, we measured the expression levels of LC3-I and LC3-II. In the four HCC cell lines tested, we found significant induction of LC3-II with sorafenib at a clinically relevant dose indicating that sorafenib increases autophagosome formation in HCC cell lines (Figure 1a). However, the expression level of Atg5, an essential factor for autophagosome formation, was not affected by sorafenib. Furthermore, sorafenib induced the formation of LC3-II in a time-dependent manner (Figure 1b, *Left*). Notably, the level of p62, a major selective substrate for autophagy that is incorporated into autophagosomes through direct binding to LC3, was decreased with sorafenib treatment. The p62 inhibition was inversely correlated with higher autophagic activity. The expression level of Beclin 1 and Atg5 were increased slightly with longer durations of sorafenib treatment (Figure 1b, *left*). To analyze the effect of sorafenib on autophagic flux, we further co-treated PLC5 cells with sorafenib and chloroquine (CQ). CQ is an autophagy inhibitor that blocks lysosome–autophagosome fusion and subsequent lysosomal protein degradation by raising lysosomal pH level. Sorafenib inhibited CQ-induced p62 and increased the level of the membrane-bound form of LC3 (LC3-II) compared to CQ alone (Figure 1b, *middle*). In addition to CQ, we used another inhibitor of autophagy, bafilomycin A1, to validate the autophagic effect of sorafenib. Combination of sorafenib and A1 induced more LC3-II production than A1 alone in PLC5 and SK-Hep1 (Figure 1b, *right*). Most importantly, both A1 and CQ significantly reduced the effect of sorafenib on cell viability. Moreover, we monitored the number of autophagosomes formed on exposure to sorafenib. Using electron microscopy, apparent autophagic vacuoles that indicate autophagosomes and late-stage autolysosomes were observed in sorafenib-treated PLC5 cells (Figure 1c). The revealed autophagosomes contained undigested cytoplasmic components such as mitochondria and fragments of endoplasmic reticulum. As autophagy is characterized by the

formation of acidic vesicular organelles (AVOs), we then stained PLC5 cells with acridine orange (AO) to measure sorafenib-induced autophagy. Protonated AO becomes trapped on the low pH side of the membrane barrier leading to its accumulation in acidic organelle structures. As shown in Figure 1d, protonated AO dye fluoresced bright red in sorafenib-treated PLC5 cells. In contrast, no distinct AO-R was observed in non-treated cells. Together, these results confirmed that sorafenib induced autophagy in HCC cell lines.

Sorafenib disrupts the Beclin 1-Mcl-1 complex through inhibition of the p-STAT3-related signaling pathway. To elucidate the molecular mechanism by which sorafenib induces autophagy in HCC cell lines, we next assayed potential targets of sorafenib involved in the regulation of this autophagic effect. Previously, RAF/MEK/ERK-mediated signaling was implicated in the sorafenib-induced anticancer effect.²⁴ Recently, other signaling pathways such as STAT3-Mcl-1 have also been reported to be involved in the effect of sorafenib.^{11,12,25,26} As shown in Figure 2a, sorafenib inhibited p-STAT3-Mcl-1 in a dose-dependent manner. It is also possible that sorafenib affects other apoptosis-related molecules in HCC cell lines. We found that the p-Akt/mTOR-related signaling pathway did not participate in the sorafenib-induced molecular events (Figure 2b). The expression statuses of p-Akt (T308)/Akt, p-mTOR (S2481)/mTOR, p-S6/S6, 4EBP1 and TSC1 were not affected by sorafenib treatment. As expected, sorafenib inactivated ERK at a higher dose (10 μ M). Beclin 1 (the mammalian ortholog of yeast Atg6), a Bcl-2-homology domain 3 (BH3)-only protein, is a key factor in the autophagy process. Beclin 1-containing complex (also called PI3K complex III), which contains Vps34, Vps15, UVRAG and inhibitory Bcl-2/Bcl-XL, contributes to vesicle nucleation in the initial step of autophagy.^{18,27} Recently, Mcl-1, an anti-apoptotic Bcl-2 homolog, has been reported to have a vital role in the regulation of autophagy. The degradation of Mcl-1 relieves Beclin 1 and thus promotes the formation of the nucleated core complex.²³ To determine whether sorafenib induces autophagy via this mechanism, we investigated the association between Mcl-1 and Beclin 1. As shown in Figure 2c, sorafenib significantly disrupts the interactions between Mcl-1 and Beclin 1. Treatment of sorafenib at 20 μ M for 16 or 48 h diminished the interactions between Mcl-1 and Beclin 1 (Figure 2c, *middle upper*). Considering that high-dose sorafenib significantly affected the expression level of Mcl-1, we also examined the association status between Beclin 1 and Mcl-1 with lower concentration of sorafenib (10 μ M). The decreased level of Mcl-1 in IP-Beclin 1-containing complex was also found in sorafenib-treated PLC5 cells (Figure 2c, *middle lower*). In addition, we also analyzed the protein–protein interactions between Beclin 1 and Mcl-1 by immunoprecipitating Mcl-1. We found that sorafenib reduced the interactions between Beclin 1 and Mcl-1. (Figure 2c, *right*). These data imply that sorafenib inhibits the expression of Mcl-1 via its transcription factor, STAT3, thereby relieving inhibition of Beclin 1 and promoting further formation of autophagosomes. Notably, Beclin 1 and its other inhibitors such as Bcl-XL were not affected by

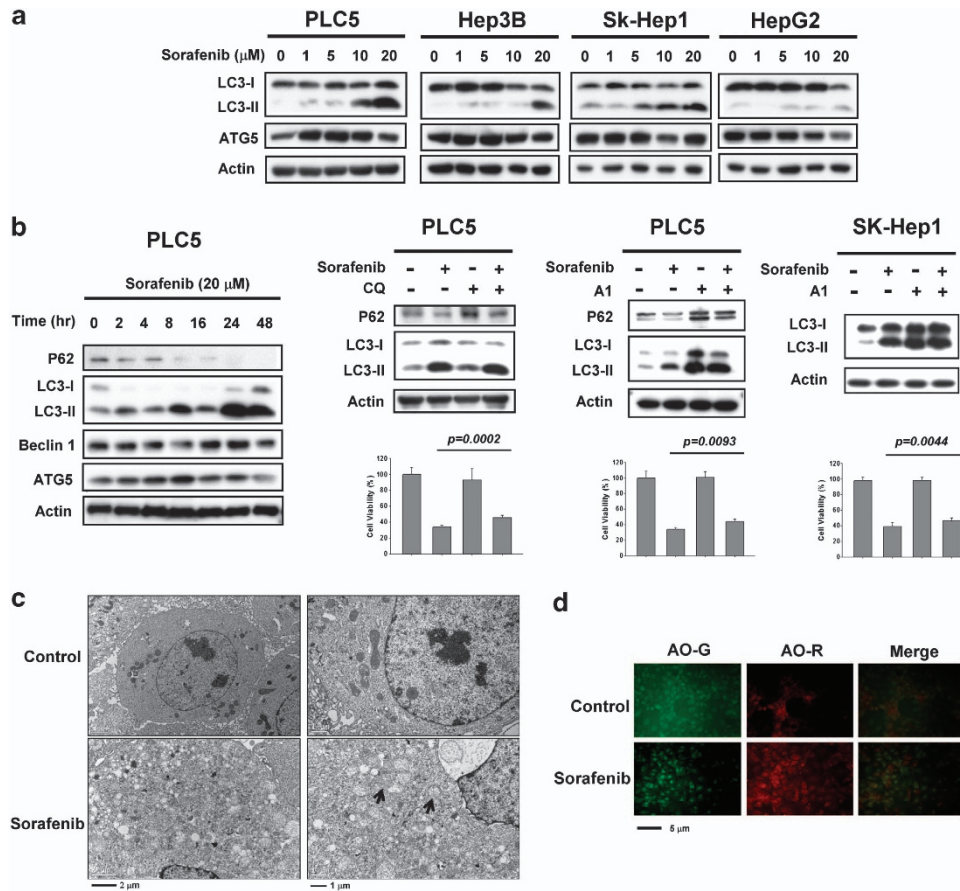


Figure 1 Sorafenib induces autophagy in HCC cells. (a) Sorafenib induces the conversion of LC3 in a dose-dependent manner. PLC5, Hep3B, SK-Hep1 and HepG2 were exposed to sorafenib at the indicated doses for 16 h and the expression levels of LC3-II were analyzed by western blot. (b) Time-dependent effect of sorafenib on autophagy-related proteins. PLC5 cells were exposed to 20 μ M sorafenib for various periods of time (left). Sorafenib activates autophagic flux in PLC5 cells (middle). Western blot showing P62 degradation and LC3 lipidation in PLC5 cells treated with sorafenib and/or lysosomal inhibitor. The cells were treated with or without 20 μ M sorafenib in the presence or absence of 10 μ M chloroquine (CQ) for 16 h. PLC5 or SK-Hep1 cells were treated with or without 20 μ M sorafenib in the presence or absence of 20 nM bafilomycin A1 (A1) for 16 h (right). The effect of CQ or A1 on cell viability was performed in MTT assay. (c) Transmission electron microscopy (TEM) images showing autophagosome (arrow) formation in PLC5 cells treated with 20 μ M sorafenib for 16 h. (d) Images of acridine orange (AO) staining of HCC cells after 16 h treatment with 20 μ M sorafenib as detected by fluorescence microscopy. AO-R indicates acidic vesicular organelle formation

sorafenib (Figure 2c, left). These results imply that sorafenib induces STAT3-dependent inhibition of Mcl-1, hence relieving its association with Beclin 1 to activate autophagy in HCC cell lines.

SHP-1-dependent inhibition of STAT3 mediates autophagic cell death induced by sorafenib. To further clarify the molecular mechanism by which sorafenib induces autophagy in HCC cell lines, we next investigated whether the SHP-1/STAT3 signaling pathway has a part in sorafenib-induced autophagy. First, we assessed the effect of inhibition of p-STAT3 on autophagy. Both sorafenib and STAT3 inhibitor III, WP1066, treatment resulted in significant conversion from LC3-I to LC-II (Figure 3a, top). Notably, this specific STAT3 inhibitor (WP1066) induced an evident amount of LC-II suggesting that inhibition of STAT3 signaling prompts autophagy in HCC cells. On the other hand, PLC5 cells with ectopic expression of STAT3 were insensitive to sorafenib-induced autophagy (Figure 3a, bottom). Together, our results suggest a potential interplay whereby sorafenib

induces an autophagic effect via inactivation of STAT3. It is important to note that sorafenib inhibits the STAT3-related signaling pathway through increasing SHP-1 phosphatase activity,^{12,14} meaning that activated SHP-1 may also be involved in sorafenib-induced autophagy. As demonstrated in Figure 3b, silencing SHP-1 with specific siRNA significantly restored the expression level of LC-II under sorafenib treatment. These data indicate that the SHP-1/STAT3-related pathway also has a vital role in sorafenib-induced autophagy.

The results shown in Figure 2c confirmed that sorafenib disrupts the interaction between Mcl-1 and Beclin 1 and suggest that relieving Beclin 1 is involved in sorafenib-induced autophagy. To further validate the role of Mcl-1 and Beclin 1 in sorafenib-induced autophagy, we assayed overexpression of Mcl-1 and knockdown of Beclin 1, respectively. Importantly, the expression level of LC-II was almost completely abolished in PLC5 cells expressing ectopic Mcl-1 (Figure 3c). Sorafenib can not induce potent autophagy in the presence of Mcl-1. Additionally, silencing Beclin 1 in HCC cells also inhibited sorafenib-induced autophagy (Figure 3d, upper). Notably,

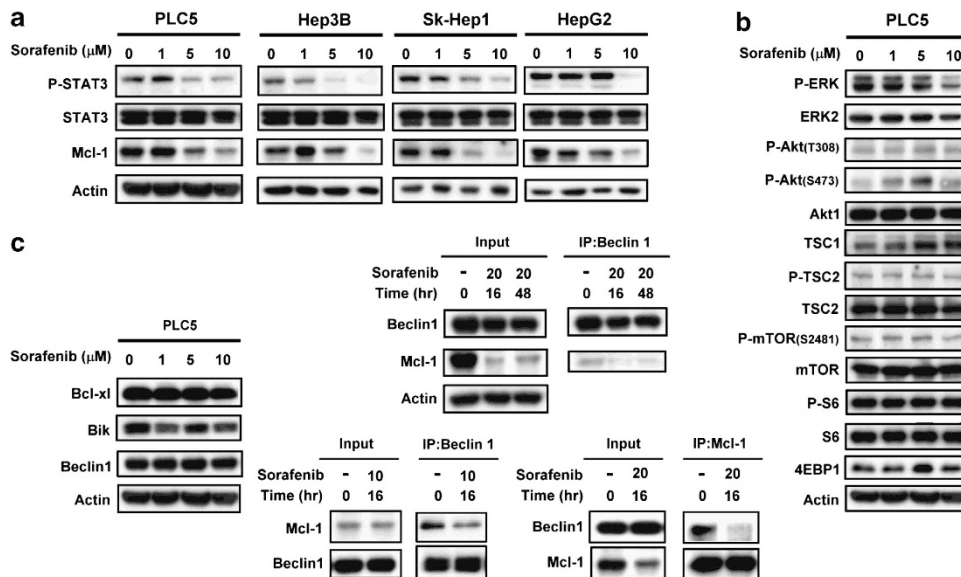


Figure 2 Sorafenib disrupts the Beclin 1–Mcl-1-complex through inhibition of the p-STAT3-related signaling pathway. (a) Effects of sorafenib on STAT3-related proteins in HCC cells. The cells were treated with sorafenib at the indicated dose for 16 h. (b) Effects of sorafenib on the Akt/mTOR-related signaling pathway in PLC5 cells. The cells were treated with sorafenib at the indicated dose for 16 h. Sorafenib does not affect the amount of Bcl-xl, Bik and Beclin 1. Sorafenib induces the disassociation of Beclin 1 and Mcl-1 (middle). Beclin 1 was immunoprecipitated from PLC5 cells treated with 10 or 20 μ M sorafenib at 16 h or 48 h and analyzed for the presence of Mcl-1 and Beclin 1. Mcl-1 was immunoprecipitated from PLC5 cells treated with 20 μ M sorafenib at 16 h and analyzed for the presence of Mcl-1 and Beclin 1 (right)

silencing of Beclin 1 reversed sorafenib-induced cell toxicity as evident by MTT assay (Figure 3d, lower). There was decreasing conversion of LC3-I to LC3-II in the absence of Beclin 1, which indicates that free-form Beclin 1 is a determinant of sorafenib-induced autophagy. Together these results confirm that SHP-1/STAT3-dependent signaling is involved in sorafenib-induced autophagy, suggesting that STAT3-driven Mcl-1 was also inhibited, resulting in the release of Beclin 1, allowing Beclin 1 to form a core complex with other interaction proteins for autophagosome formation.

SC-59, a kinase-independent derivative of sorafenib, induces more autophagic cell death than sorafenib.

Recently, we applied the kinase-independent mechanism of SC-1 as a molecular basis from which to develop a novel class of SHP-1 activators.^{14,15} The replacement of N-methylpicolinamide with a phenylcyano group abolished kinase activity while retaining phospho-STAT3 repressive activity. Screening of these derivatives revealed that SC-59 in particular had a potent autophagic effect in HCC cell lines. To further address the effect of SC-59 on autophagic cell death, here we performed more specific assays to validate the molecular mechanism of SC-59. The difference in chemical structure between sorafenib and SC-59 is shown in Figure 4a. The kinase-independent characteristic of SC-59 was confirmed by Raf-1 activity (Figure 4a, right). In four HCC cell lines, SC-59 showed more significant cytotoxicity than sorafenib in a dose-escalation manner (Figure 4b). In addition, SC-59 exhibited better effects than sorafenib on apoptosis in a dose-dependent manner (Figure 4c). SC-59 demonstrated substantial apoptosis in a dose-dependent manner. SC-59 also induced the inhibition of p-STAT3 and

potential autophagy as a result of more conversion to LC3-II (Figure 4d, upper). At the same dose (10 μ M), SC-59 displayed a more potent effect on autophagy than sorafenib in all four HCC cell lines (Figure 4d, lower). We also found distinct evidence of autophagosome formation using electron microscopy (Figure 4e, upper) and AO staining (Figure 4e, lower) after SC-59 treatment. We found that SC-59 also induced autophagy with co-treatment of CQ. Importantly, SC-59-induced cell viability change was reversed by adding CQ (Figure 4f, left). Further, A1 also rescued the effect of SC-59 on cell toxicity in PLC5 and SK-Hep1 (Figure 4f, right). Therefore, we propose that the anti-HCC effect of SC-59 is correlated with autophagic cell death.

Relieving Beclin 1 results in SC-59-induced autophagy via a SHP-1/STAT3/Mcl-1-dependent signaling pathway.

To investigate the molecular mechanism by which SC-59 induces an anti-HCC effect, we assayed the impact of SHP-1/STAT3-dependent signaling on SC-59-induced autophagy. First, we investigated whether inactivation of STAT3 was related to SC-59-induced autophagy. Both SC-59 and WP1066 showed the conversion from LC3-I to LC3-II (Figure 5a, left). In contrast, SC-59 did not induce evident LC3-II in PLC5 cells ectopically expressing STAT3 (Figure 5a, left). Meanwhile, SC-59 lost its autophagic effect in the absence of SHP-1. We did not find distinct expression of LC3-II in PLC5 cells with silenced SHP-1 (Figure 5a, right). As activation of SHP-1 has been found to be part of a major kinase-independent mechanism of action of this sorafenib derivative, we further assayed the effect of SC-59 on SHP-1 phosphatase activity. As expected, we observed that SC-59 increased SHP-1 phosphatase activity in a dose-dependent

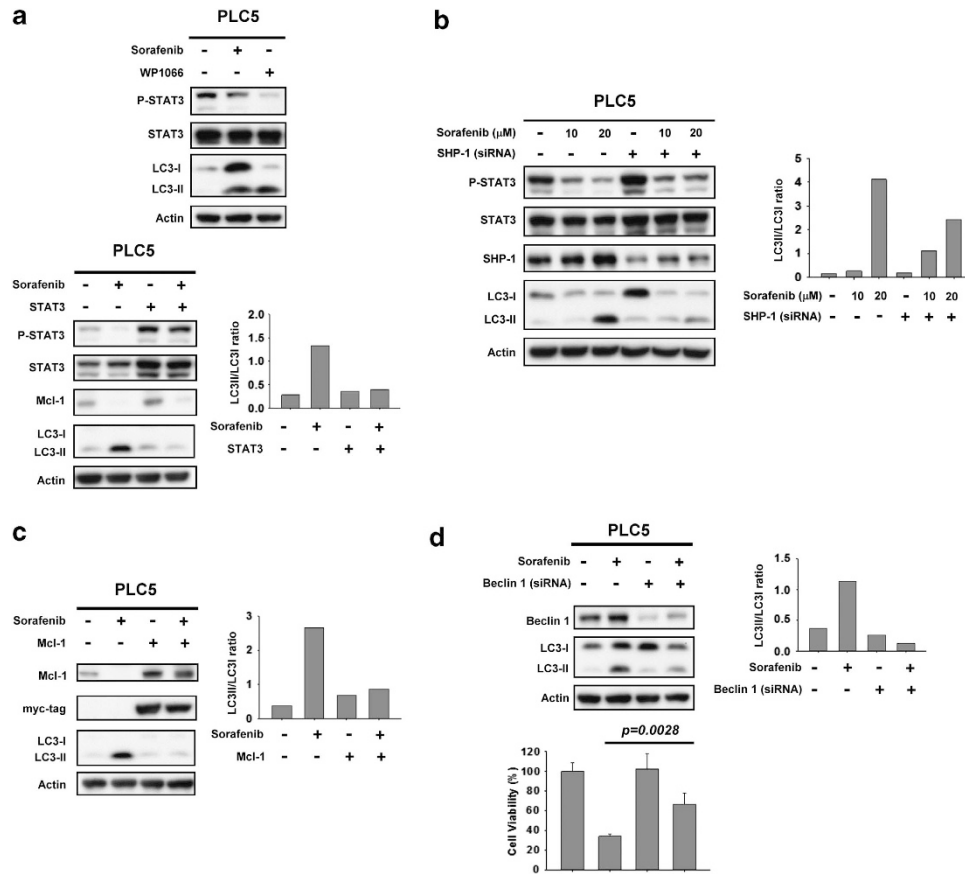


Figure 3 Inhibition of p-STAT3 is involved in sorafenib-induced autophagy through the induction of SHP phosphatase activity. (a) Specific inhibition of p-STAT3 induces significant autophagic activity. WP1066, a specific inhibitor of STAT3, induces autophagy in PLC5 cells (top). Cells ectopically expressing STAT3 were treated with sorafenib at 10 μ M for 16 h and the level of expression of LC3-II was measured (bottom). (b) Silencing SHP-1 by siRNA reduces the effect of sorafenib on p-STAT3 and LC3-II in HCC cells. PLC5 cells were transfected with control siRNA or SHP-1 siRNA for 24 h and then treated with sorafenib for 16 h. (c) Effects of Mcl-1 on autophagy induced by sorafenib in HCC cells. Wild-type PLC5 or PLC5 transiently transfected with Mcl-1 were treated with sorafenib at 10 μ M for 16 h. (d) Silencing Beclin 1 by siRNA reduces the effects of sorafenib on LC3-II in HCC cells. PLC5 cells were transfected with control siRNA or Beclin 1 siRNA for 24 h, then treated with sorafenib at 10 μ M for 16 h. The effect of siBeclin 1 on cell viability was demonstrated in MTT assay

manner in both PLC5 cells and SHP-1-containing IP complex (Figure 5b). Notably, SC-59 induced more potent phosphatase activity than sorafenib incubation *in vitro*.

As sorafenib disrupted the interaction between Beclin 1 and Mcl-1, we further investigated whether SC-59 also affects this association to induce autophagy. As shown in Figure 5c, SC-59 treatment decreased the level of Mcl-1 in Beclin 1-containing complex, suggesting that SC-59 releases more free-form Beclin 1 through Mcl-1 inhibition and thus promotes autophagy. To further confirm the roles of Mcl-1 and Beclin 1 in this autophagic effect, we transfected either ectopic Mcl-1 or siBeclin 1 into PLC5 cells to observe the effect of SC-59 on autophagy. Both overexpression of Mcl-1 and silencing Beclin 1 in HCC cells almost fully restored the conversion from LC3-I to LC3-II induced by SC-59, indicating that the inhibitory effect of Mcl-1 is a key basis for autophagy induced by sorafenib and its derivatives (Figure 5d, Upper).

The knockdown of Beclin 1 also significantly reversed the effect of SC-59 on cell survival in PLC5 cells (Figure 5d, lower). To examine the effect of sorafenib and SC-59 on Mcl-1, we investigated the effect of sorafenib or SC-59 on the transcription of Mcl-1. Our data showed that sorafenib or

SC-59 significantly decreased mRNA levels of Mcl-1 in a time-dependent manner (Figure 5e, right). Notably, the treatment of sorafenib or SC-59 did not alter the degradation of Mcl-1 significantly (Figure 5e, left).

Taken together, we propose that sorafenib and its derivative, SC-59, inhibit the expression of Mcl-1 and further release Beclin 1 to form a nucleated core complex through a SHP-1/STAT3-dependent signaling pathway. Moreover, based on the premise that SC-59 acts in a kinase-independent manner, we propose a specific role for SHP-1/STAT3 in autophagic cell death that accounts for the observation of more cytotoxicity and LC-II in SC-59 than sorafenib-treated cells.

Sorafenib and SC-59 induce significant tumor growth inhibition via SHP-1-dependent autophagic cell death.

To verify tumor growth inhibition by sorafenib and its derivative SC-59, we applied these two drugs to HCC-bearing mice and evaluated the biological effect *in vivo*. SC-59 showed more potent tumor growth inhibition than sorafenib at the same dose (20 mg/kg/day) (Figure 6a, left). Autophagic vesicles were observed in tumors treated

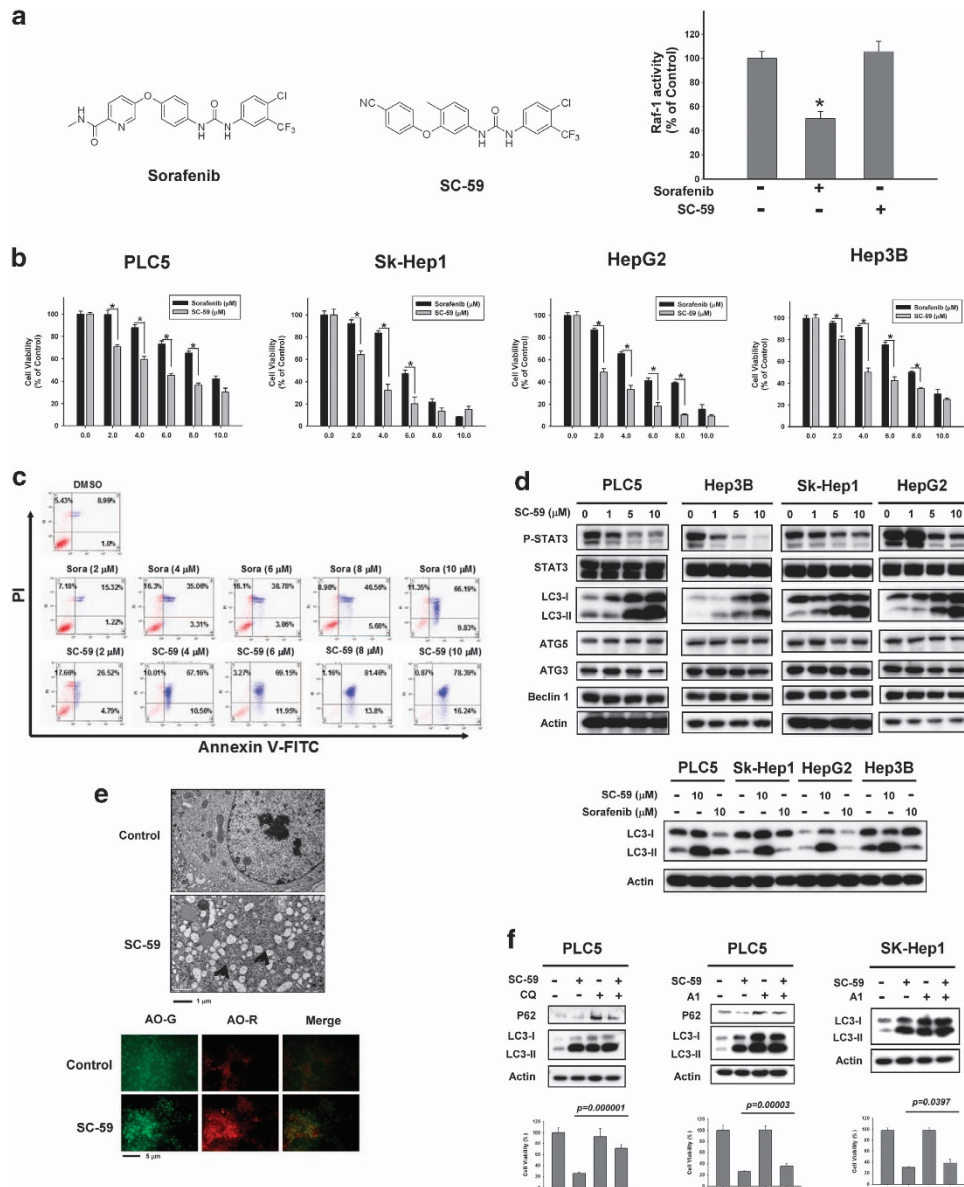
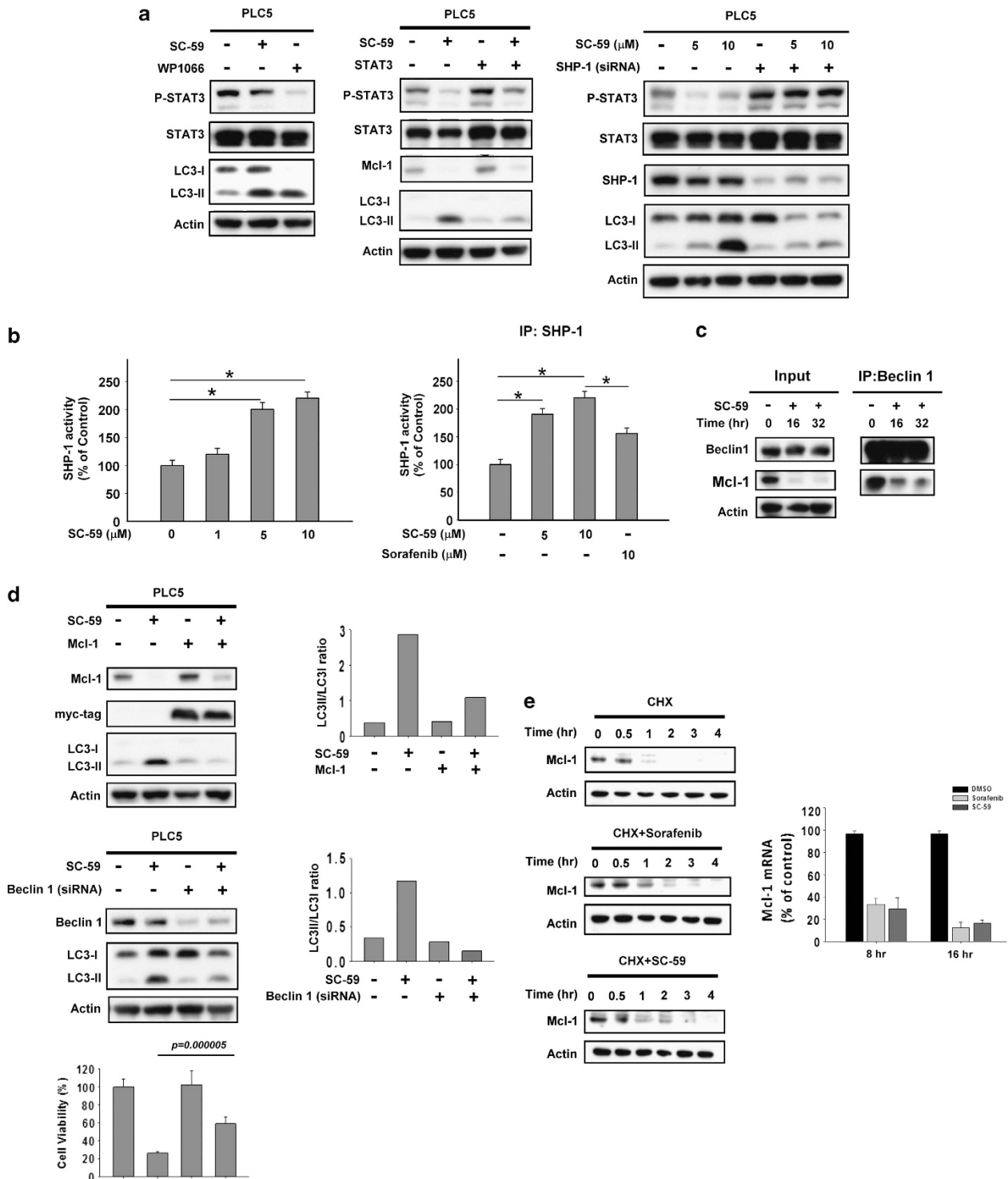


Figure 4 SC-59, a kinase-independent derivative of sorafenib, is a more effective anticancer agent than sorafenib in HCC cells. **(a)** Chemical structures of sorafenib and SC-59 (left). Effect of sorafenib and SC-59 on Raf-1 activity. Hep3B cells were treated with sorafenib or SC-59 at 10 μ M for 24 h (right). Columns, mean; bars, S.D. ($n=3$). * $P<0.05$. **(b)** The cell viability of sorafenib and SC-59 in four HCC cell lines. The cells were treated with sorafenib or SC-59 at indicated dose for 48 h and cell viability was assessed by MTT assay. Columns, mean; bars, S.D. ($n=8$). * $P<0.05$. **(c)** Both sorafenib and SC-59 induced significant apoptosis in a dose-dependent manner. The early and late apoptosis was observed in sorafenib or SC-59-treated PLC5 cells. **(d)** SC-59 downregulates p-STAT3 and increases LC3-II in HCC cells (upper). The cells were treated with SC-59 at indicated dose for 16 h. SC-59 induces more LC3-II than sorafenib. The cells were treated with 10 μ M SC-59 or sorafenib for 16 h (lower). **(e)** Transmission electron microscopy images showing autophagosome (arrow) formation in PLC5 cells treated with 10 μ M SC-59 for 16 h (upper). fluorescence microscopy images of AO staining in HCC cells after 16 h treatment with 10 μ M SC-59 (lower). AO-R indicates acidic vesicular organelle formation, which demonstrates the formation of autolysosomes. **(f)** SC-59 activates autophagic flux in PLC5 and SK-Hep1 (left). Western blot showing P62 degradation and LC3 lipidation in PLC5 cells treated with SC-59 and/or lysosomal inhibitor. The cells were treated with or without 10 μ M SC-59 in the presence or absence of 10 μ M chloroquine (CQ) for 16 h. PLC5 or SK-Hep1 cells were treated with or without 10 μ M SC-59 in the presence or absence of 20 nM Bafilomycin A1 (A1) for 16 h (right). The effect of CQ or A1 on cell viability was performed in MTT assay

with sorafenib and SC-59 by TEM (Figure 6a, right). These data indicate sorafenib and SC-59 induced significant autophagy *in vivo*. Importantly, we found significant inhibition of p-STAT3 and Mcl-1 in both the sorafenib and SC-59-treated tumor samples (Figure 6b, left). The conversion from LC3-I to LC3-II was also demonstrated in both treatments. The kinase-independent derivative SC-59, showed a

stronger effect on the SHP-1/STAT3-related signaling pathway, and displayed more potent autophagic cell death through an increased level of LC3-II (quantitative data in Figure 6b, middle). We also found more significant induction of SHP-1 activity in SC-59-treated tumor samples (Figure 6c). These data indicate that both sorafenib and SC-59 show an important anti-HCC effect *in vivo*; and the



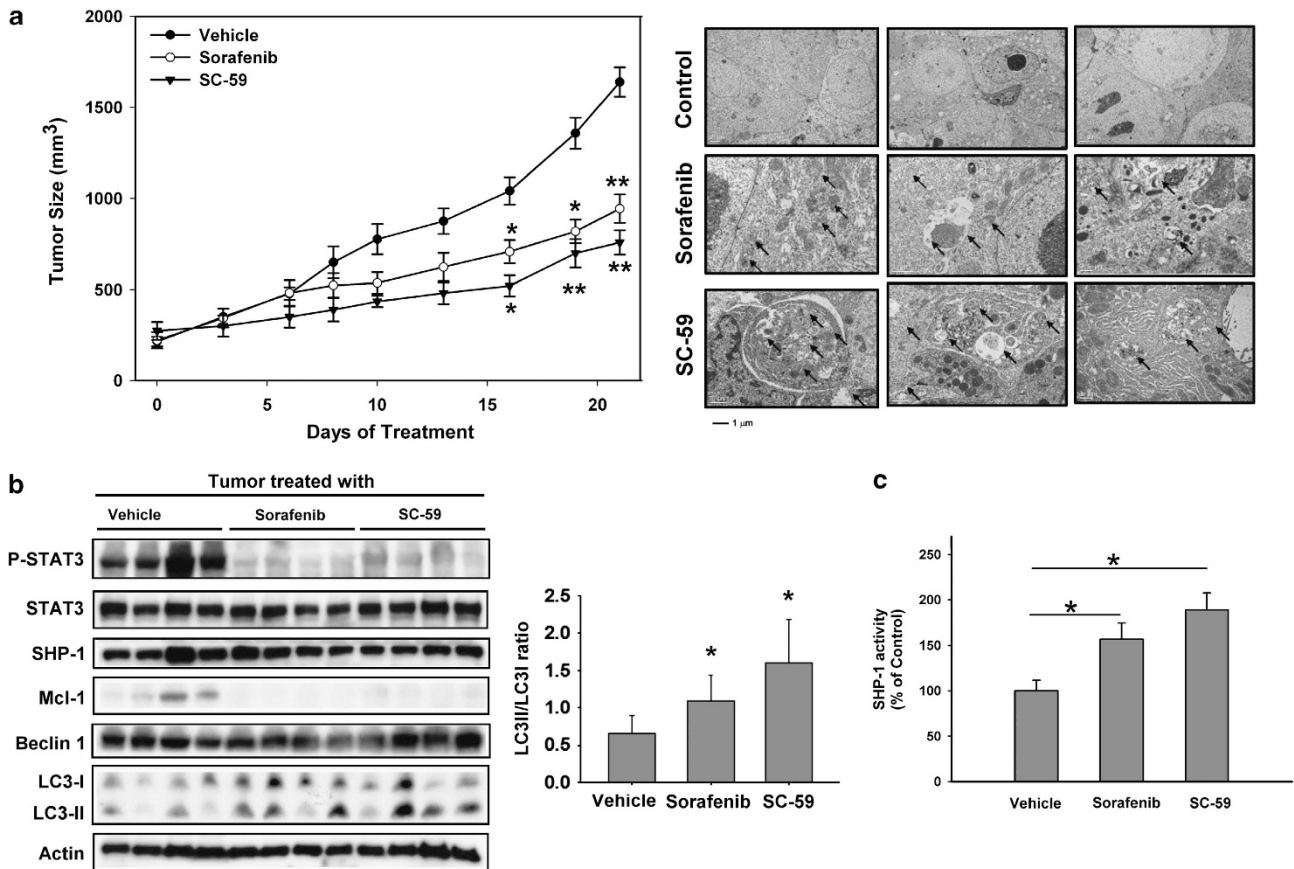


Figure 6 SC-59 exhibits more potent tumor growth inhibition and reveals significant SHP-1 activity and higher levels of expression of LC3-II than sorafenib in HCC-bearing mice. (a) Sorafenib (20 mg/kg) and SC-59 (20 mg/kg) inhibit PLC5 tumor growth (left). Points, mean; bars, S.E. ($n = 10$). * $P < 0.05$. ** $P < 0.01$. SC-59 and sorafenib-induced autophagosomes were demonstrated in the tumor sample (right). (b) Western blot analysis of p-STAT3, STAT3, SHP-1, Mcl-1, Beclin 1 and LC3 in PLC5 tumors. (c) SHP-1 activity in PLC5 tumors. Columns, mean; bars, S.D. ($n = 10$). * $P < 0.05$

critical role of SHP-1/STAT3-related signaling in autophagic cell death was also proved in this preclinical animal model.

Discussion

In this study, we proposed a molecular mechanism for the induction of autophagy by sorafenib. First, we validated the effect of sorafenib on autophagy by measuring: (1) the conversion of the cytoplasmic form of LC3 (LC3-I) to pre-autophagosomal/autophagosomal membrane-bound LC3 (LC3-II); (2) the autophagic degradation of p62; (3) electron microscopy of autophagosomes and (4) AO staining to monitor AVOs. Next, we further confirmed that sorafenib disrupts the interaction between Beclin 1 and Mcl-1, suggesting that more relieved Beclin 1 is available to promote autophagosome formation. STAT3-dependent inhibition of Mcl-1 caused the release of Beclin 1 from the Beclin 1-Mcl-1 complex as demonstrated in sorafenib-treated PLC5 cells (Figure 2c). Importantly, both overexpression of Mcl-1 and silencing of Beclin 1 almost completely abolished autophagy induced by sorafenib (Figures 3c and d). Based on the results obtained with SC-59, a kinase-independent derivative of sorafenib, we further confirmed the molecular effect of SHP-1/STAT3-related signaling on sorafenib-induced

autophagy. SC-59 had a more potent effect on SHP-1 phosphatase activity and higher levels of autophagy compared to sorafenib (Figure 4). Knockdown of SHP-1 in HCC cells inhibited the conversion of LC3-I to LC3-II, suggesting that activated SHP-1 has a vital role in sorafenib/SC-59-induced autophagy. In the HCC xenograft, significant tumor growth inhibition was observed in mice treated with sorafenib or SC-59. The more potent SC-59 showed significant induction of autophagic marker, LC3-II, and SHP-1 phosphatase activity *in vivo* (Figure 6). These results suggest that the SHP-1/STAT3/Mcl-1 signaling pathway takes part in sorafenib-induced autophagic cell death via relieving of Beclin 1 both *in vitro* and *in vivo*.

Previously, sorafenib has been reported to induce both apoptosis and autophagy in human HCC cells via ERK1/2-independent ER stress.²⁸ This report suggests that sorafenib-induced autophagy alleviates ER stress-induced cell death and has a role in the molecular basis of resistance. Consequently, the combination of sorafenib with the autophagy inhibitor chloroquine (CQ) produced more pronounced tumor suppression in HCC both *in vivo* and *in vitro*. It has also been reported that autophagic activity triggered by sorafenib conferred a survival advantage to HCC cells.²⁹ However, based on our results for the kinase-independent derivative of

sorafenib, SC-59, we propose that activated autophagic flux is correlated with a potent apoptotic effect.

Beclin 1, carrying one BH3 domain, is a key initial protein involved in autophagy and the Beclin 1-containing core complex conducts the nucleation step in autophagosome formation.^{30,31} Importantly, anti-apoptotic proteins of the Bcl-2 family such as Bcl-2 and Bcl-xL can interact with Beclin 1 at residues 114–123 within the BH3 domain and inhibit the function of the Vps34–UVRAG–Beclin 1 nucleated core complex.^{22,27,32,33} Moreover, the phosphorylation of Beclin 1 at T119 within BH3 domain by DAPK was reported to dissociate Beclin 1 from inhibitory Bcl-xL and promote autophagic activity.³⁴ In addition, Mcl-1 also has an inhibitory effect on the Beclin 1-associated core complex. For example, the expression of Mcl-1 protected against the combination of lapatinib and obatoclox lethality. Lapatinib and obatoclox-initiated autophagy was found to depend on NOXA-mediated displacement of the pro-survival BCL-2 family member, MCL-1, from beclin 1.³⁵ In our data, we propose that degradation of Mcl-1 is crucial for sorafenib-induced autophagy by releasing Beclin 1. This effect also determines autophagic cell death in the kinase-independent derivative, SC-59.

Previously, we proposed that the SHP-1/STAT3-related signaling pathway is a major target for inhibition of Mcl-1 and promotion of cell death in HCC.²⁶ However, little is known about the interplay between STAT3 and autophagy. The inhibition of STAT3 and mTOR were reported to be involved in telomere 3'-overhang-specific DNA oligonucleotide (T-oligo)-induced cancer cell death.³⁶ In contrast, ROS-dependent activated STAT3 was also observed in cells treated with rapamycin or under starvation to promote the autophagic process.³⁷ We found that WP1066, a specific JAK/STAT3 inhibitor, as well as sorafenib can induce a significant expression level of LC3-II, and that, ectopic expression of STAT3 can further restore sorafenib-induced autophagy, which indicates that inhibition of p-STAT3 has a vital role in autophagic activity. In addition, SHP-1, a negative regulator of STAT3, is also implicated in the promotion of sorafenib-induced autophagy. Silencing SHP-1 almost fully abolished the conversion of LC3 induced by sorafenib (Figure 3b). Moreover, the higher levels of autophagy induced by SC-59 were correlated to anti-HCC effect *in vitro* and *in vivo*.

In this study, we proposed a molecular mechanism for the induction of autophagic cell death by sorafenib in HCC. Both sorafenib and its derivative induced the inhibition of Mcl-1 via a SHP-1/STAT3-related pathway and released Beclin 1 to promote autophagosome formation. This study thus suggests that the disassociation of Mcl-1 and Beclin 1 manages sorafenib-induced autophagy in HCC.

Materials and Methods

Reagents and antibodies. Sorafenib (Nexavar) was kindly provided by Bayer Pharmaceuticals (West Haven, CT, USA). For *in vitro* studies, sorafenib at various concentrations was dissolved in DMSO and then added to the cells in Dulbecco's modified Eagle's medium (DMEM) containing 5% fetal bovine serum (FBS). Chloroquine, Bafilomycin A1, cycloheximide and WP1066 were purchased from Sigma (Deisenhofen, Germany). Antibodies for immunoblotting such as Akt1, anti-pERK-1/2 ERK2 were purchased from Santa Cruz Biotechnology (San Diego, CA, USA). SHP-1 antibody was purchased from Abcam (Cambridge, UK). Other antibodies such as Bcl-xL, Bik, p-STAT3 (Tyr705), STAT3, p-Akt (Ser473), p-Akt (Thr308), LC3, Mcl-1, myc-tag, Beclin 1, Atg5, Atg3, P62, TSC1, p-TSC2, TSC2,

p-mTOR (S2481), mTOR, p-S6, S6, p-4EBP1 and 4EBP1 were purchased from Cell Signaling (Danvers, MA, USA).

Cell culture and western blot analysis. The PLC/PRF/5 (PLC5), Sk-Hep-1, Hep3B and HepG2 cell lines were obtained from American Type Culture Collection (Manassas, VA, USA). The cells were maintained in DMEM supplemented with 10% FBS, 100 units/ml penicillin G, 100 μ g/ml streptomycin sulfate and 25 μ g/ml amphotericin B in a humidified incubator at 37 °C in an atmosphere of 5% CO₂ in air. Lysates of HCC cells treated with drugs at the indicated concentrations for various periods of time will be prepared for immunoblotting of LC3, p-STAT3, STAT3, and so on. Western blot analysis was performed as previously reported.³⁸

Autophagy analysis. The following three methods were used to assess drug-induced autophagic cell death: (1) western blot analysis of microtubule-associated protein-1 light chain 3 (LC3 II) as described previously;^{16,39,40} (2) electron microscopy: samples were fixed with 2.5% glutaraldehyde solution buffer in PBS at 4 °C for 1 h, postfixed in 1% osmium tetroxide solution at 4 °C for 3 h, dehydrated in graded concentrations of ethanol and embedded in LR white resin. Ultrathin sections (70 nm) were examined with a JEOL JEM-1400EX electron microscope (JEOL Inc., Tokyo, Japan) at 120 Kv; (3) immunofluorescence of acridine orange: HCC cells were grown on coverslips. After being washed with PBS, cells were treated with 20 μ M sorafenib or 10 μ M SC-59 for 16 h, fixed with ice-cold 4% paraformaldehyde for 30 min at room temperature, then stained with acridine orange (5 μ g/ml) for 5 min at room temperature. The cells were examined under a Leica DM2500 fluorescence microscope (Leica Microsystems GmbH, Wetzlar, Germany).

Cell viability assay. HCC cells including PLC5 and SK-Hep1 were seeded in 96-well plate at a density of 5000 cells per well. The cells were treated with sorafenib (20 μ M) or SC-59 (10 μ M) with indicated condition including over-expression of Mcl-1, knockdown of Beclin 1 or co-treatment with Bafilomycin A1 or CQ for 16 h. The cell viability was measured by MTT assay.

Annexin V/PI staining. PLC5 cells were treated with indicated dose for 48 h and collected for Annexin V/PI-double staining. The analysis of annexin V binding was carried out with the Annexin V-FITC according to the manufacturer's instructions (eBioscience, San Diego, CA, USA). Briefly, the cells were incubated with sorafenib or SC-59 for 48 h and then collected, washed twice with cold PBS, centrifuged at 1500 r.p.m. for 5 min and resuspended in 1 \times Annexin V binding buffer at a concentration of 10⁶ cells/ml. Annexin V-FITC (5 μ l) and PI (25 μ g/ml) were added into cell extract and incubated for 15 min at room temperature in the dark. The stained sample were analyzed with Gallios Flow Cytometry (Beckman Coulter Inc., Fullerton, CA, USA) based on the manufacturer's instructions.

Real-time PCR. Total RNA was isolated from PLC5 with RNA extraction kit (Ambion-Invitrogen, Lennik, Belgium) and cDNA was prepared from 2.5 μ g RNA using SuperScript.

Vilo cDNA Synthesis Kit by the manufacturer's instructions (Invitrogen, Carlsbad, CA, USA). Oligonucleotide sequences were used as follows: GAPDH, 5'-CGA CCACTTTGTCAAGCTCA-3' (sense) and 5'-AGGGGTCTACATGGAACATG-3' (anti-sense); Mcl-1: 5'-CTTGCCACTTGCTTTCTGG-3' (sense) and 5'-CAAGGC ATGCTTCGGAAC-3' (antisense). The SYBR Green PCR reagent was used for quantitative PCR by the manufacturer's instructions (ABI, Carlsbad, CA, USA).

Gene knockdown using siRNA. Smart pool siRNA reagents, including a control (D-001810-10), SHP-1 and Beclin 1 were all purchased from Dharmacon (Chicago, IL, USA). The procedure was as described previously.^{39,41}

PLC5 with ectopic expression of STAT3 and Mcl-1. STAT3 cDNA (KIAA1524) and Mcl-1 was purchased from Addgene plasmid repository (<http://www.addgene.org/>). PLC5 cells with stable expression of STAT3 or transient expression of Mcl-1 were then treated with drugs, harvested and processed for western blot analysis as described previously.⁴²

Activity of Raf-1 and SHP-1. Tyrosine Phosphatase Assay Kit (R-22067) was used for SHP-1 activity assay (Molecular Probes, Invitrogen). The Raf-1 kinase cascade assay kit (Upstate-Millipore, Billerica, MA, USA) was used to

examine the Raf-1 kinase activity. Both the assays were conducted according to the manufacturer's instructions.

Xenograft tumor growth. Male NCr athymic nude mice (5–7 weeks of age) were obtained from the National Laboratory Animal Center (Taipei, Taiwan). All experimental procedures using these mice were performed in accordance with protocols approved by the Institutional Laboratory Animal Care and Use Committee of National Taiwan University. Each mouse was inoculated s.c. in the dorsal flank with 1×10^6 PLC5 cells suspended in 0.1 ml of serum-free medium containing 50% Matrigel (BD Biosciences, Bedford, MA, USA). When the tumors reached 200–300 mm³, mice received sorafenib tosylate (20 mg/kg) or SC-59 (20 mg/kg) p.o. once daily. Controls received vehicle. Tumors will be measured weekly using calipers and their volumes calculated using the following standard formula: width² × length × 0.52.

Statistical analysis. Comparisons of mean values were performed using the independent samples *t*-test in SPSS for Windows 11.5 software (SPSS, Inc., Chicago, IL, USA).

Conflict of Interest

Dr. Ann-Lii Cheng serves as a consultant and a member of the speaker's bureau for Bayer-Schering. All other authors declare no conflict of interest.

Acknowledgements. This study was supported by grants, NTUH 101P01 from National Taiwan University Hospital (K-F C), NSC99-2314-B-002-017-MY2 (K-F C) and NSC 100-2325-B-002-032 (K-F C) from the National Science Council, Taiwan.

- Kao JH, Chen DS. Changing disease burden of hepatocellular carcinoma in the Far East and Southeast Asia. *Liver Int* 2005; **25**: 696–703.
- Wang SH, Yeh SH, Lin WH, Wang HY, Chen DS, Chen PJ. Identification of androgen response elements in the enhancer I of hepatitis B virus: a mechanism for sex disparity in chronic hepatitis B. *Hepatology* 2009; **50**: 1392–1402.
- Kao JH, Chen PJ, Chen DS. Recent advances in the research of hepatitis B virus-related hepatocellular carcinoma: epidemiologic and molecular biological aspects. *Adv Cancer Res* 2010; **108**: 21–72.
- Yeh SH, Chen PJ. Gender disparity of hepatocellular carcinoma: the roles of sex hormones. *Oncology* 2010; **78**: 172–179.
- Chen PJ, Yeh SH, Liu WH, Lin CC, Huang HC, Chen CL *et al*. Androgen pathway stimulates MicroRNA-216a transcription to suppress the tumor suppressor in lung cancer-1 gene in early hepatocarcinogenesis. *Hepatology* 2012; **56**: 632–643.
- Forner A, Llovet JM, Bruix J. Chemoembolization for intermediate HCC: is there proof of survival benefit? *J Hepatol* 2012; **56**: 984–986.
- Bruix J, Llovet JM. HCC surveillance: who is the target population? *Hepatology* 2003; **37**: 507–509.
- Shen YC, Hsu C, Cheng AL. Molecular targeted therapy for advanced hepatocellular carcinoma: current status and future perspectives. *J Gastroenterol* 2010; **45**: 794–807.
- Llovet JM, Ricci S, Mazzaferro V, Hilgard P, Gane E, Blanc JF *et al*. Sorafenib in advanced hepatocellular carcinoma. *N Engl J Med* 2008; **359**: 378–390.
- Cheng AL, Kang YK, Chen Z, Tsao CJ, Qin S, Kim JS *et al*. Efficacy and safety of sorafenib in patients in the Asia-Pacific region with advanced hepatocellular carcinoma: a phase III randomised, double-blind, placebo-controlled trial. *Lancet Oncol* 2009; **10**: 25–34.
- Rosmorduc O, Desbois-Mouthon C. Targeting STAT3 in hepatocellular carcinoma: sorafenib again. *J Hepatol* 2011; **55**: 957–959.
- Tai WT, Cheng AL, Shiau CW, Huang HP, Huang JW, Chen PJ *et al*. Signal transducer and activator of transcription 3 is a major kinase-independent target of sorafenib in hepatocellular carcinoma. *J Hepatol* 2011; **55**: 1041–1048.
- Zhang Q, Wang HY, Marzec M, Raghunath PN, Nagasawa T, Wasik MA. STAT3- and DNA methyltransferase 1-mediated epigenetic silencing of SHP-1 tyrosine phosphatase tumor suppressor gene in malignant T lymphocytes. *Proc Natl Acad Sci USA* 2005; **102**: 6948–6953.
- Chen KF, Tai WT, Hsu CY, Huang JW, Liu CY, Chen PJ *et al*. Blockade of STAT3 activation by sorafenib derivatives through enhancing SHP-1 phosphatase activity. *Eur J Med Chem* 2012; **55**: 220–227.
- Chen KF, Tai WT, Huang JW, Hsu CY, Chen WL, Cheng AL *et al*. Sorafenib derivatives induce apoptosis through inhibition of STAT3 independent of Raf. *Eur J Med Chem* 2011; **46**: 2845–2851.
- Mizushima N. Autophagy: process and function. *Genes Dev* 2007; **21**: 2861–2873.

- David R. Metabolism: keeping fit with autophagy. *Nat Rev Mol Cell Biol* 2012; **13**: 136.
- Kang R, Zeh HJ, Lotze MT, Tang D. The Beclin 1 network regulates autophagy and apoptosis. *Cell Death Differ* 2011; **18**: 571–580.
- Bergmann A. Autophagy and cell death: no longer at odds. *Cell* 2007; **131**: 1032–1034.
- Codogno P, Mehrpour M, Proikas-Cezanne T. Canonical and non-canonical autophagy: variations on a common theme of self-eating? *Nat Rev Mol Cell Biol* 2012; **13**: 7–12.
- Maiuri MC, Zalckvar E, Kimchi A, Kroemer G. Self-eating and self-killing: crosstalk between autophagy and apoptosis. *Nat Rev Mol Cell Biol* 2007; **8**: 741–752.
- Pattingre S, Tassa A, Qu X, Garuti R, Liang XH, Mizushima N *et al*. Bcl-2 antiapoptotic proteins inhibit Beclin 1-dependent autophagy. *Cell* 2005; **122**: 927–939.
- Germain M, Nguyen AP, Le Grand JN, Arbour N, Vanderluit JL, Park DS *et al*. MCL-1 is a stress sensor that regulates autophagy in a developmentally regulated manner. *EMBO J* 2011; **30**: 395–407.
- Liu L, Cao Y, Chen C, Zhang X, McNabola A, Wilkie D *et al*. Sorafenib blocks the RAF/MEK/ERK pathway, inhibits tumor angiogenesis, and induces tumor cell apoptosis in hepatocellular carcinoma model PLC/PRF/5. *Cancer Res* 2006; **66**: 11851–11858.
- Blechacz BR, Smoot RL, Bronk SF, Werneburg NW, Sirica AE, Gores GJ. Sorafenib inhibits signal transducer and activator of transcription-3 signaling in cholangiocarcinoma cells by activating the phosphatase shatterproof 2. *Hepatology* 2009; **50**: 1861–1870.
- Chen KF, Tai WT, Liu TH, Huang HP, Lin YC, Shiau CW *et al*. Sorafenib overcomes TRAIL resistance of hepatocellular carcinoma cells through the inhibition of STAT3. *Clin Cancer Res* 2010; **16**: 5189–5199.
- Marquez RT, Xu L. Bcl-2:Beclin 1 complex: multiple mechanisms regulating autophagy/apoptosis toggle switch. *Am J Cancer Res* 2012; **2**: 214–221.
- Shi YH, Ding ZB, Zhou J, Hui B, Shi GM, Ke AW *et al*. Targeting autophagy enhances sorafenib lethality for hepatocellular carcinoma via ER stress-related apoptosis. *Autophagy* 2011; **7**: 1159–1172.
- Shimizu S, Takehara T, Hikita H, Kodama T, Tsunematsu H, Miyagi T *et al*. Inhibition of autophagy potentiates the antitumor effect of the multikinase inhibitor sorafenib in hepatocellular carcinoma. *Int J Cancer* 2012; **131**: 548–557.
- Maiuri MC, Criollo A, Tasdemir E, Vicencio JM, Tajeddine N, Hickman JA *et al*. BH3-only proteins and BH3 mimetics induce autophagy by competitively disrupting the interaction between Beclin 1 and Bcl-2/Bcl-X(L). *Autophagy* 2007; **3**: 374–376.
- Maiuri MC, Criollo A, Kroemer G. Crosstalk between apoptosis and autophagy within the Beclin 1 interactome. *EMBO J* 2010; **29**: 515–516.
- Ku B, Woo JS, Liang C, Lee KH, Jung JU, Oh BH. An insight into the mechanistic role of Beclin 1 and its inhibition by prosurvival Bcl-2 family proteins. *Autophagy* 2008; **4**: 519–520.
- Maiuri MC, Le Toumelin G, Criollo A, Rain JC, Gautier F, Juin P *et al*. Functional and physical interaction between Bcl-X(L) and a BH3-like domain in Beclin-1. *EMBO J* 2007; **26**: 2527–2539.
- Zalckvar E, Berissi H, Eisenstein M, Kimchi A. Phosphorylation of Beclin 1 by DAP-kinase promotes autophagy by weakening its interactions with Bcl-2 and Bcl-XL. *Autophagy* 2009; **5**: 720–722.
- Tang Y, Hamed HA, Cruickshanks N, Fisher PB, Grant S, Dent P. Obatoclox and lapatinib interact to induce toxic autophagy through NOXA. *Mol Pharmacol* 2012; **81**: 527–540.
- Yokoyama T, Kondo Y, Kondo S. Roles of mTOR and STAT3 in autophagy induced by telomere 3' overhang-specific DNA oligonucleotides. *Autophagy* 2007; **3**: 496–498.
- Yoon S, Woo SU, Kang JH, Kim K, Kwon MH, Park S *et al*. STAT3 transcriptional factor activated by reactive oxygen species induces IL6 in starvation-induced autophagy of cancer cells. *Autophagy* 2010; **6**: 1125–1138.
- Chen KF, Yeh PY, Yeh KH, Lu YS, Huang SY, Cheng AL. Down-regulation of phospho-Akt is a major molecular determinant of bortezomib-induced apoptosis in hepatocellular carcinoma cells. *Cancer Res* 2008; **68**: 6698–6707.
- Itakura E, Mizushima N. p62 Targeting to the autophagosome formation site requires self-oligomerization but not LC3 binding. *J Cell Biol* 2011; **192**: 17–27.
- Tsujimoto Y, Shimizu S. Another way to die: autophagic programmed cell death. *Cell Death Differ* 2005; **12**(Suppl 2): 1528–1534.
- Tai WT, Cheng AL, Shiau CW, Liu CY, Ko CH, Lin MW *et al*. Dovitinib induces apoptosis and overcomes sorafenib resistance in hepatocellular carcinoma through SHP-1-mediated inhibition of STAT3. *Mol Cancer Ther* 2012; **11**: 452–463.
- Chen KF, Yeh PY, Hsu C, Hsu CH, Lu YS, Hsieh HP *et al*. Bortezomib overcomes tumor necrosis factor-related apoptosis-inducing ligand resistance in hepatocellular carcinoma cells in part through the inhibition of the phosphatidylinositol 3-kinase/Akt pathway. *J Biol Chem* 2009; **284**: 11121–11133.



Cell Death and Disease is an open-access journal published by Nature Publishing Group. This work is licensed under the Creative Commons Attribution-NonCommercial-No Derivative Works 3.0 Unported License. To view a copy of this license, visit <http://creativecommons.org/licenses/by-nc-nd/3.0/>